

Thieno[2,3-*d*]pyrimidine-Based Positive Allosteric Modulators of Human Mas-Related G Protein-Coupled Receptor X1 (MRGPRX1)

Ilyas Berhane, Niyada Hin, Ajit G. Thomas, Qian Huang, Chi Zhang, Vijayabhaskar Veeravalli, Ying Wu, Justin Ng, Jesse Alt, Camilo Rojas, Hiroe Hihara, Mika Aoki, Kyoko Yoshizawa, Tomoki Nishioka, Shuichi Suzuki, Shao-Qiu He, Qi Peng, Yun Guan, Xinzhong Dong, Srinivasa N. Raja, Barbara S. Slusher, Rana Rais,* and Takashi Tsukamoto*



Cite This: <https://doi.org/10.1021/acs.jmedchem.1c01709>



Read Online

ACCESS |



Metrics & More



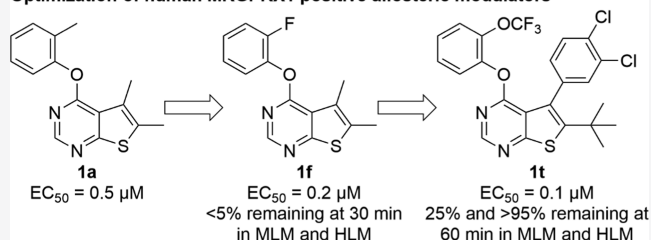
Article Recommendations



Supporting Information

ABSTRACT: Mas-related G protein-coupled receptor X1 (MRGPRX1) is a human sensory neuron-specific receptor and potential target for the treatment of pain. Positive allosteric modulators (PAMs) of MRGPRX1 have the potential to preferentially activate the receptors at the central terminals of primary sensory neurons and minimize itch side effects caused by peripheral activation. Using a high-throughput screening (HTS) hit, a series of thieno[2,3-*d*]pyrimidine-based molecules were synthesized and evaluated as human MRGPRX1 PAMs in HEK293 cells stably transfected with human *MrgprX1* gene. An iterative process to improve potency and metabolic stability led to the discovery of orally available 6-(*tert*-butyl)-5-(3,4-dichlorophenyl)-4-(2-(trifluoromethoxy)phenoxy)thieno[2,3-*d*]pyrimidine (**1t**), which can be distributed to the spinal cord, the presumed site of action, following oral administration. In a neuropathic pain model induced by sciatic nerve chronic constriction injury (CCI), compound **1t** (100 mg/kg, po) reduced behavioral heat hypersensitivity in humanized MRGPRX1 mice, demonstrating the therapeutic potential of MRGPRX1 PAMs in treating neuropathic pain.

Optimization of human MRGPRX1 positive allosteric modulators



INTRODUCTION

Mas-related G protein-coupled receptor X1 (MRGPRX1) is expressed specifically in the small-diameter dorsal root ganglion (DRG) sensory neurons and is implicated in the modulation of nociception.¹ MRGPRX1 has gained increased interest as a promising therapeutic target partly based on the analgesic effects of BAM8-22 (Figure 1),² a proteolytic product derived from proenkephalin A with full agonist activity at human MRGPRX1 and its closest rodent orthologues, mouse MRGPRC11 and rat MRGPRC.³ DRG sensory neurons have

both centrally and peripherally projecting axons. The analgesic effects of MRGPRX1 agonists are thought to be partially mediated by downstream inhibition of N-type calcium channels resulting in reduced synaptic inputs to the spinal cord dorsal horn neurons.⁴ On the other hand, activation of peripheral MRGPRX1 localized in nerve terminals in the skin may generate an itch sensation.⁵ These dual effects produced by direct activation of MRGPRX1 at the central and peripheral terminals of DRG neurons may limit the therapeutic utility of small-molecule orthosteric MRGPRX1 agonists^{6,7} for systemic treatment. Interestingly, BAM22, another endogenous peptide-based MRGPRX1 agonist, was found to be upregulated at spinal dorsal horn during persistent pain after nerve injury or tissue inflammation, while it was undetectable in the skin.⁸ These findings have presented a unique therapeutic opportunity for positive allosteric modulators (PAMs) of MRGPRX1, which can potentiate the agonist effects of the

BAM8-22

Val-Gly-Arg-Pro-Glu-Trp-Trp-Met-Asp-Tyr-Gln-Lys-Arg-Tyr-Gly

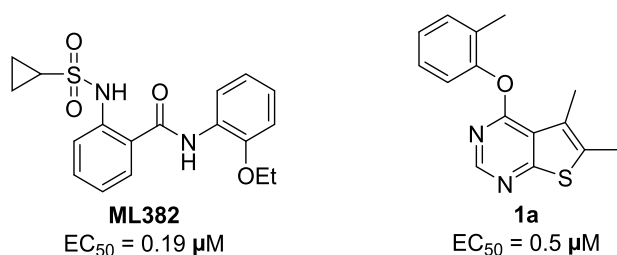


Figure 1. Chemical structures of BAM8-22, ML382, and compound **1a**.

Received: October 1, 2021

endogenous agonist at the central terminals of sensory neurons without activating peripheral MRGPRX1, thus minimizing itch side effects.

2-[(Cyclopropylsulfonyl)amino]-*N*-(2-ethoxyphenyl)-benzamide, also known as ML382, is a prototype MRGPRX1 PAM identified by the Molecular Libraries Probe Production Centers Network (MLPCN).⁹ ML382 was found to inhibit pain hypersensitivity after injury following intrathecal injection, and systemic administration of ML382 did not elicit itch side effects.⁸ These findings confirm the presence of endogenous MRGPRX1 agonists in the spinal cord under persistent pain conditions and demonstrate the therapeutic potential of MRGPRX1 PAMs as novel analgesic agents devoid of the peripheral itch side effects. However, ML382 produces analgesic effects only when injected intrathecally presumably due to its poor distribution to the spinal cord, limiting its therapeutic utility in treating chronic neuropathic pain. This prompted us to explore structurally distinct MRGPRX1 PAMs with improved pharmacokinetic (PK) properties and *in vivo* analgesic efficacy following oral administration.

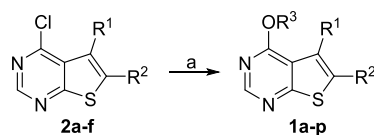
To this end, we conducted high-throughput screening of Eisai's compound library in HEK293 cells stably transfected with human MRGPRX1 using FLIPR Calcium 4 Assay Kit (Molecular Devices) to measure intracellular calcium responses.¹⁰ We identified 5,6-dimethyl-4-(*o*-tolylxy)thieno[2,3-*d*]pyrimidine **1a** as a potent MRGPRX1 PAM with an EC₅₀ value of 0.5 μM. Although compound **1a** is less potent than ML382, its lack of a hydrogen-bond donor prompted us to use this hit compound as a molecular template in an attempt to identify MRGPRX1 PAMs with improved pharmacokinetic properties. Here, we describe the design, synthesis, and structure–activity relationships (SAR) of a new series of human MRGPRX1 PAMs using compound **1a** as a molecular template. Our optimization efforts aimed at improving not only MRGPRX1 PAM potency but also metabolic stability led to the discovery of an orally available MRGPRX1 PAM, potentially valuable as a new lead for treating neuropathic pain.

CHEMISTRY

Compounds **1a–p** were synthesized by reacting 4-chloro-thieno[2,3-*d*]pyrimidines **2a–f** with various phenols pretreated with NaH (Scheme 1).

Compound **1q** was synthesized in three steps starting with a one-pot synthesis of thieno[2,3-*d*]pyrimidin-4-ol **4** via the Gewald reaction.¹¹ Compound **4** was subsequently converted to 4-chloro derivative **5** by treating with phosphoryl chloride. Nucleophilic substitution with 2-fluorophenol afforded the desired product **1q**.

Scheme 1. Synthesis of Compounds **1a–p**^a



R¹ = H, CH₃, or CF₃; R² = H, CH₃, or C(CH₃)₃;
R³ = Ph, 2-MePh, 3-MePh, 4-MePh, 2-FPh, 3-FPh,
4-FPh, 2-CF₃Ph, 3-CF₃Ph, or 4-CF₃Ph
The individual molecular structures **1a–p** are shown
in Table 1.

^aReagents and conditions: (a) R³OH, NaH, dimethylformamide (DMF), 0 °C to room temperature (rt), 33–93%.

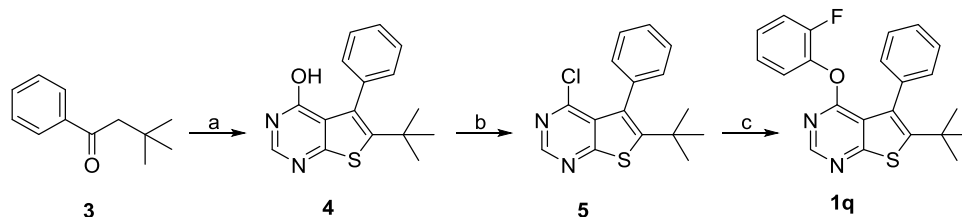
Although the synthetic route developed for compound **1q** (Scheme 2) described above takes only three steps to the desired product, it suffered from the poor yield in the first step involving the four-component reaction, presumably due to the steric hindrance by the *tert*-butyl group in starting material **3**. This prompted us to explore alternative routes to compounds **1r–t** containing a *tert*-butyl group at the 6-position. As shown in Scheme 3, 6-(*tert*-butyl)-4-chloro-thieno[2,3-*d*]pyrimidine **2f** was first converted into the 6-methoxy derivative **6**. Compound **6** was brominated at its 5-position by *N*-bromosuccinimide (NBS) to give compound **7**. The Suzuki coupling of compound **7** with aryl boronic acids gave compounds **8a–b**. After converting **8a–b** to 4-chloro derivative **10a–b**, the desired product **1r–t** was obtained by reacting them with either 2-fluorophenol or 2-trifluoromethoxyphenol.

RESULTS AND DISCUSSION

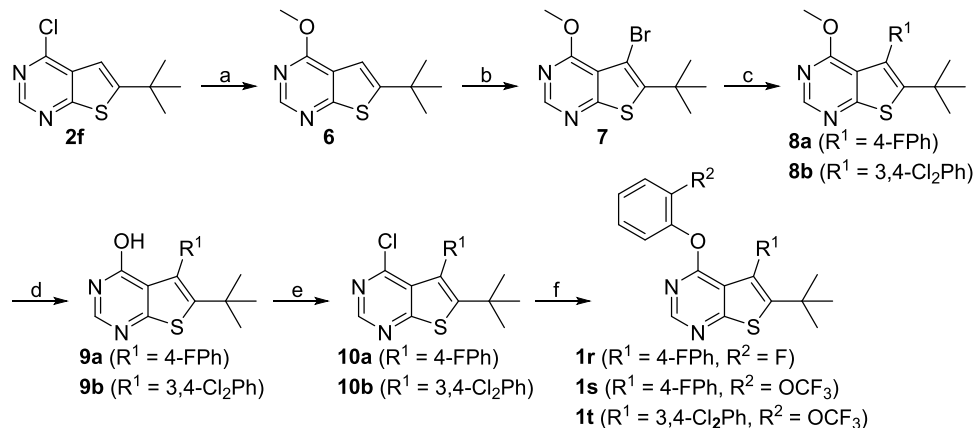
In vitro experiments measuring PAM activity at MRGPRX1 were performed with an FLIPR assay using HEK293 cells stably transfected with MRGPRX1 in the presence of EC₂₀ (5–15 nM) of BAM8-22, an MRGPRX1 agonist devoid of opioid receptor affinity displayed by BAM22. The results are summarized in Table 1. All of the compounds with a submicromolar EC₅₀ value displayed E_{max} ≥ 95% relative to the maximum response achieved by BAM8-22 alone. It should be noted that compound **1b** was also identified as an active allosteric MRGPRX1 activator by the NIH Molecular Libraries Probe Centers Network (MLPCN).¹² In our assay, compound **1b** displayed a 20-fold lower potency compared to compound **1a**, indicating an important role played by the 5- and 6-methyl groups of **1a** in the PAM potency. Thus, we tested 5,6-dimethylthieno[2,3-*d*]pyrimidine derivatives **1c–k** possessing various phenoxy groups at the 4-position. Compound **1c** containing an unsubstituted phenoxy group showed a 4-fold loss in potency compared to **1b**. *m*-Tolylxy and *p*-tolylxy derivatives **1d** and **1e** displayed substantially lower potency. We also explored fluoro and trifluoromethyl substitutions at the 4-phenoxy group in a systematic manner (compounds **1f–k**). As observed with methyl substitutions, ortho-substituted derivatives **1f** and **1i** exhibited greater potency than *meta*- and *para*-substituted derivatives **1g–h** and **1j–k**. Among these, compound **1f** containing a 2-fluorophenoxy group at the 4-position showed the most potent PAM activity.

In the subsequent set of compounds, we retained the 2-fluorophenoxy group at the 4-position and modified the 5- and 6-positions of the thieno[2,3-*d*]pyrimidine ring. Compound **1l** unsubstituted at the 5- and 6-positions showed much weaker potency. This is consistent with the substantial loss of potency observed in compound **1b** compared to **1c**. The removal of one methyl group either from 5- or 6-position from **1a** also resulted in a loss of potency as seen in compounds **1m** and **1n**. Replacement of the 5-methyl group with a trifluoromethyl group (compound **1o**) did not improve the potency either. Interestingly, the introduction of a *tert*-butyl group into the 6-position (compounds **1p–r**) led to submicromolar potency.

In the last stage, we incorporated a 2-(trifluoromethyl)-phenoxy group into the 4-position of the 6-(*tert*-butyl)thieno[2,3-*d*]pyrimidine scaffold as seen in compounds **1s** and **1t**. Compound **1t** represents one of the most potent MRGPRX1 PAMs within this series. We also confirmed that compound **1t** has no intrinsic agonist activity at concentrations up to 100 μM

Scheme 2. Synthesis of Compound 1q^a

^aReagents and conditions: (a) ethylcyanoacetate, S₈, formamide, L-proline, Et₂NH, 170 °C, 4%; (b) POCl₃, 100 °C, 66%; (c) 2-fluorophenol, NaH, DMF, 0 °C to rt, 40%.

Scheme 3. Synthesis of Compounds 1r–t^a

^aReagents and conditions: (a) MeONa, MeOH, 0 °C to rt, 98%; (b) NBS, AcOH, 55 °C, 85%; (c) R¹B(OH)₂, PdCl₂(PPh₃)₂, K₂CO₃, DMF, 80 °C, 92% for 8a, 75% for 8b; (d) BBr₃, dichloromethane (DCM), rt, 41% for 9a, 93% for 9b; (e) POCl₃, 110 °C, 61% for 10a, 95% for 10b; (f) 2-fluorophenol or 2-(trifluoromethoxy)phenol, NaH, DMF, 0 °C to rt, 77% for 1r, 65% for 1s, 69% for 1t.

in the absence of BAM8-22 (Supporting information Figure S1).

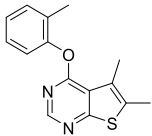
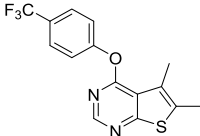
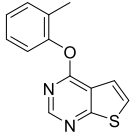
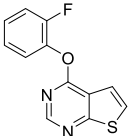
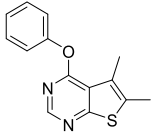
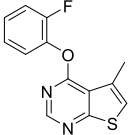
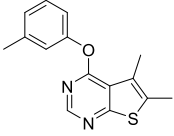
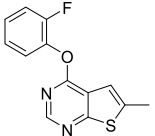
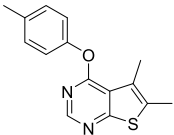
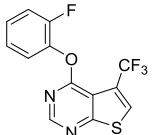
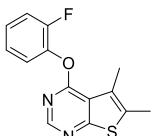
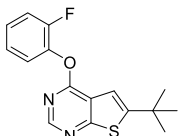
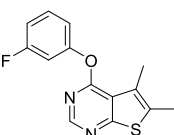
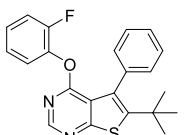
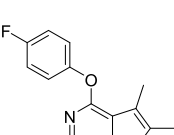
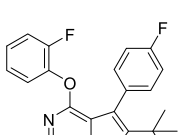
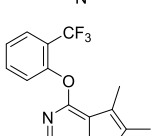
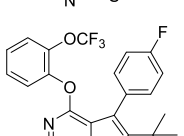
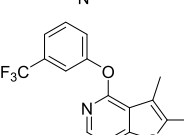
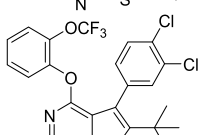
Structural optimization detailed above was guided by not only PAM potency but also metabolic stability. Table 2 summarizes the metabolic stability (% remaining after 30 and 60 min of incubation) of selected compounds in mouse and human liver microsomes. Compound 1f was extensively metabolized within 30 min in both human and mouse microsomes. Notably, the loss of the parent compound was only observed in the presence of NADPH, suggesting CYP450-mediated oxidation involved in the metabolism of 1f. Metabolite identification was attempted for compound 1f using high-resolution mass spectrometry (HR-MS) analysis. A sample from compound 1f exposed to human liver microsomes for 60 min exhibited a new peak representing [MH⁺ + 16] (291.0612), suggesting an insertion of an oxygen atom into the parent compound (Figure 2). Fragmentation of the Phase I metabolite using MS/MS spectroscopy showed a major peak for a fragment at 170.0256, corresponding to the oxidized thiophene moiety (Figure 2), indicating that the CYP450-mediated oxidation was primarily taking place on the thieno[2,3-*d*]pyrimidine moiety of compound 1f.

Compound 1o was designed to make the thieno[2,3-*d*]pyrimidine ring electron-deficient by the electron-withdrawing effects of the 5-trifluoromethyl group. Although it showed slightly better stability in human liver microsomes, it failed to show any improvement over compound 1f in mouse liver microsomes. Interestingly, compounds 1p–r possessing a *tert*-butyl group at the 6-position showed substantially improved stability in human liver microsomes, presumably

by protecting the thieno portion from oxidation. As seen with compound 1f, however, these three compounds were extensively metabolized within a period of 30 min in mouse liver microsomes. Given these species-dependent metabolic stability data, it is conceivable that another site is being metabolized in mouse liver microsomes. Indeed, upon incorporation of a 2-(trifluoromethoxy)phenoxy group into the 4-position (compound 1s), a slight improvement in stability was achieved against mouse liver microsomes. It should be also noted that compound 1s was completely stable in human liver microsomes. Finally, compound 1t, in which a 3,4-dichlorophenyl is introduced into the 5-position, showed substantial improvement in stability against mouse liver microsomes with 25% remaining at 60 min.

Given its potent PAM activity and good metabolic stability, we selected compound 1t for *in vivo* pharmacokinetic studies in mice. In addition to plasma and brain levels, we measured drug levels in the spinal cord (Figure 3), which is the putative site of action for MRGPRX1 PAMs to attenuate spinal nociceptive transmission. As shown in Table 3, substantial levels of 1t were detected in plasma ($C_{\max} = 38.98 \pm 5.06$ nmol/mL; $AUC_{0-\text{last}} = 108.53 \pm 1.18$ nmol·h/mL) following oral administration (100 mg/kg). In contrast, its distribution to the brain was substantially restricted. Compound 1t, however, was distributed to the spinal cord ($C_{\max} = 4.60 \pm 0.60$ nmol/mL; $AUC_{0-\text{last}} = 13.79 \pm 0.14$ nmol·h/mL) with a spinal cord-to-plasma ratio of 0.13. While C_{\max} in the spinal cord is more than 40-fold greater than the EC₅₀ value of compound 1t, additional studies will be required to determine the precise pharmacokinetic/pharmacodynamic (PK/PD)

Table 1. *In Vitro* Potency of Compounds 1a–t as MRGPRX1 PAMs^{ab}

Cmpd	Structure	EC ₅₀ (μM) ^a (E _{max}) ^b	Cmpd	Structure	EC ₅₀ (μM) ^a (E _{max}) ^b
1a		0.48 ± 0.04 (118%)	1k		>100
1b		14.5 ± 1.1 (88%)	1l		4.2 ± 1.1 (95%)
1c		1.6 ± 0.4 (89%)	1m		1.7 ± 0.2 (94%)
1d		25 (40%)	1n		1.5 ± 0.2 (90%)
1e		2.7 ± 1.5 (88%)	1o		2.1 ± 0.4 (94%)
1f		0.22 ± 0.02 (112%)	1p		0.32 ± 0.06 (105%)
1g		30 (55%)	1q		0.34 ± 0.07 (95%)
1h		1.1 ± 0.2 (83%)	1r		0.30 ± 0.13 (145%)
1i		0.52 ± 0.03 (95%)	1s		0.23 ± 0.05 (143%)
1j		>100	1t		0.10 ± 0.01 (114%)

^aValues are mean ± standard error of the mean (SEM) of at least three independent experiments performed in quadruplicate. ^bE_{max} values were defined as response elicited by maximum concentration of test compounds in the presence of EC₂₀ concentration of BAM8-22 normalized to that elicited by 250 nM (>EC₁₀₀) of BAM8-22 alone.

Table 2. Metabolic Stability in Mouse and Human Liver Microsomes

compd	% remaining			
	mouse		human	
	30 min	60 min	30 min	60 min
1f	<5	<5	<5	<5
1o	<5	<5	40	<5
1p	<5	<5	75	61
1q	14	<5	94	78
1r	7	<5	>95	88
1s	28	5	>95	>95
1t	58	25	>95	>95

relationship, including the evaluation of dose response and the quantification of unbound drug concentrations in the spinal cord tissues.

To assess its selectivity as a PAM, compound **1t** was tested in HEK293 cells stably expressing MRGPRX2 in the presence of EC₂₀ concentration of C48/80,¹³ a known MRGPRX2 orthosteric agonist, using Fluo-4 AM-based calcium detection assay (Supporting Information Figure S2). Compound **1t** showed no MRGPRX2 PAM activity at 5 μ M, indicating at least 50-fold selectivity for MRGPRX1. Subsequently, a broader off-target activity profile of compound **1t** was evaluated by screening against a panel of 44 selected targets (Eurofins Cerep SafetyScreen 44) recommended by major pharmaceutical companies.¹⁴ At 10 μ M, compound **1t** was found to inhibit five targets (Supporting Information Table S1) by more than 50% (50–64%) including hERG channel. Although these off-target activities were detected at a concentration 100-fold greater than its EC₅₀ value for MRGPRX1, future structural optimization efforts should aim to improve not only MRGPRX1 PAM potency but also selectivity over these targets.

To examine if compound **1t** elicits any adverse effect, spontaneous behaviors were video-recorded for 0–1 h post-drug in awake, free-moving humanized MRGPRX1 mice, in which human MRGPRX1 is specifically expressed in nociceptive DRG neurons and replacing the murine homologue, *MrgprC11*.⁸ Compared to vehicle, compound **1t** at this oral dose (100 mg/kg) caused no overt adverse effects including itch side effects as evident from the lack of spontaneous scratch bouts (Supporting Information Table S3). In the open field test, neither compound **1t** (100 mg/kg, po) nor vehicle significantly impaired exploratory performance in naïve MRGPRX1 mice compared to pre-drug (Supporting

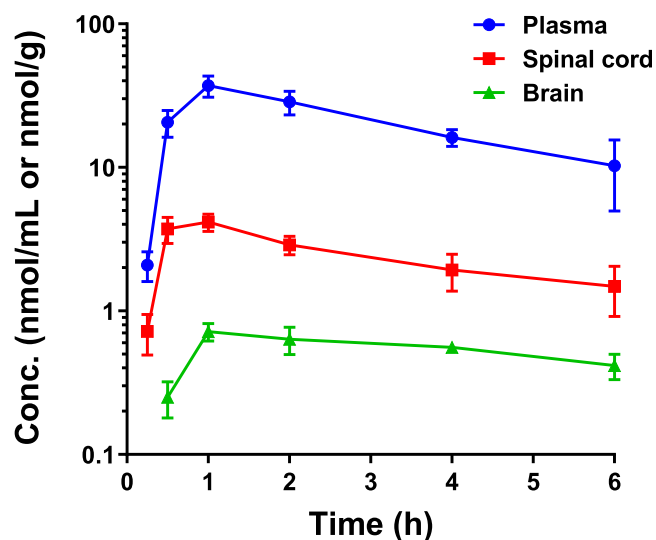


Figure 3. Plasma, spinal cord, and brain levels of compound **1t** in mice following oral administration (100 mg/kg).

Information Figure S3A–E). Furthermore, naïve MRGPRX1 mice treated with compound **1t** (100 mg/kg, po) showed no difference in performance on the rotarod test compared to the vehicle-treated group and pretreatment values (Supporting Information Figure S3F). Collectively, no signs of acute toxicity were observed after oral administration of compound **1t** (100 mg/kg) in naïve MRGPRX1 mice, presumably due to its limited penetration to the brain and/or sensory neuron-specific expression of MRGPRX1.

Compound **1t** was subsequently tested for its pain inhibitory effects *in vivo* following oral administration (100 mg/kg, po) in the sciatic nerve chronic constriction injury (CCI) model of neuropathic pain¹⁵ using humanized MRGPRX1 mice. As shown in Figure 4, sciatic nerve CCI decreased paw withdrawal latency (PWL) to radiant heat stimuli in the hind paw (left) ipsilateral to the injury on days 12 and 26 post-injury, compared to pre-injury level, suggesting heat hypersensitivity. The contralateral (right) PWL was not significantly changed after injury. Importantly, compound **1t** (100 mg/kg, po), but not vehicle, significantly increased ipsilateral PWLs from pre-drug level at 1 and 2 h post-drug on day 12 (Figure 4A) and at 2 h post-drug on day 26 post-injury (Figure 4B). There was no significant change of PWLs on the contralateral hind paw after drug treatment.

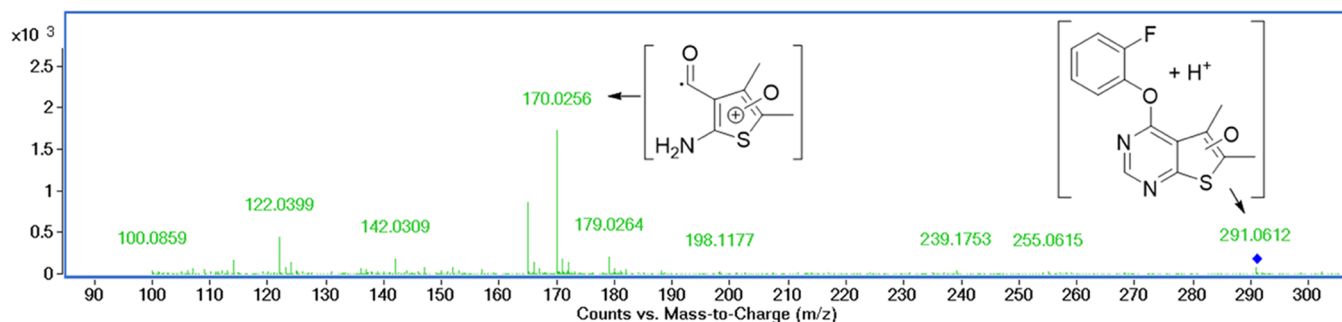


Figure 2. Identification of the major metabolite of compound **1f** incubated in human liver microsomes. MS/MS spectroscopy of the major metabolite [MH⁺ + 16] shows a fragment corresponding to the oxidized thiophenium moiety.

Table 3. *In Vivo* Pharmacokinetic Profiles of Compound 1t

	T_{\max} (h)	C_{\max} (nmol/mL or nmol*h/g)	$AUC_{0-\text{last}}$ (nmol*h/mL or nmol*h/g)	tissue-to-plasma ratio (by AUC)
plasma	1	38.98 ± 5.06	108.53 ± 1.18	
brain	1	0.82 ± 0.05	2.37 ± 0.03	2.2%
spinal cord	1	4.60 ± 0.60	13.79 ± 0.14	12.7%

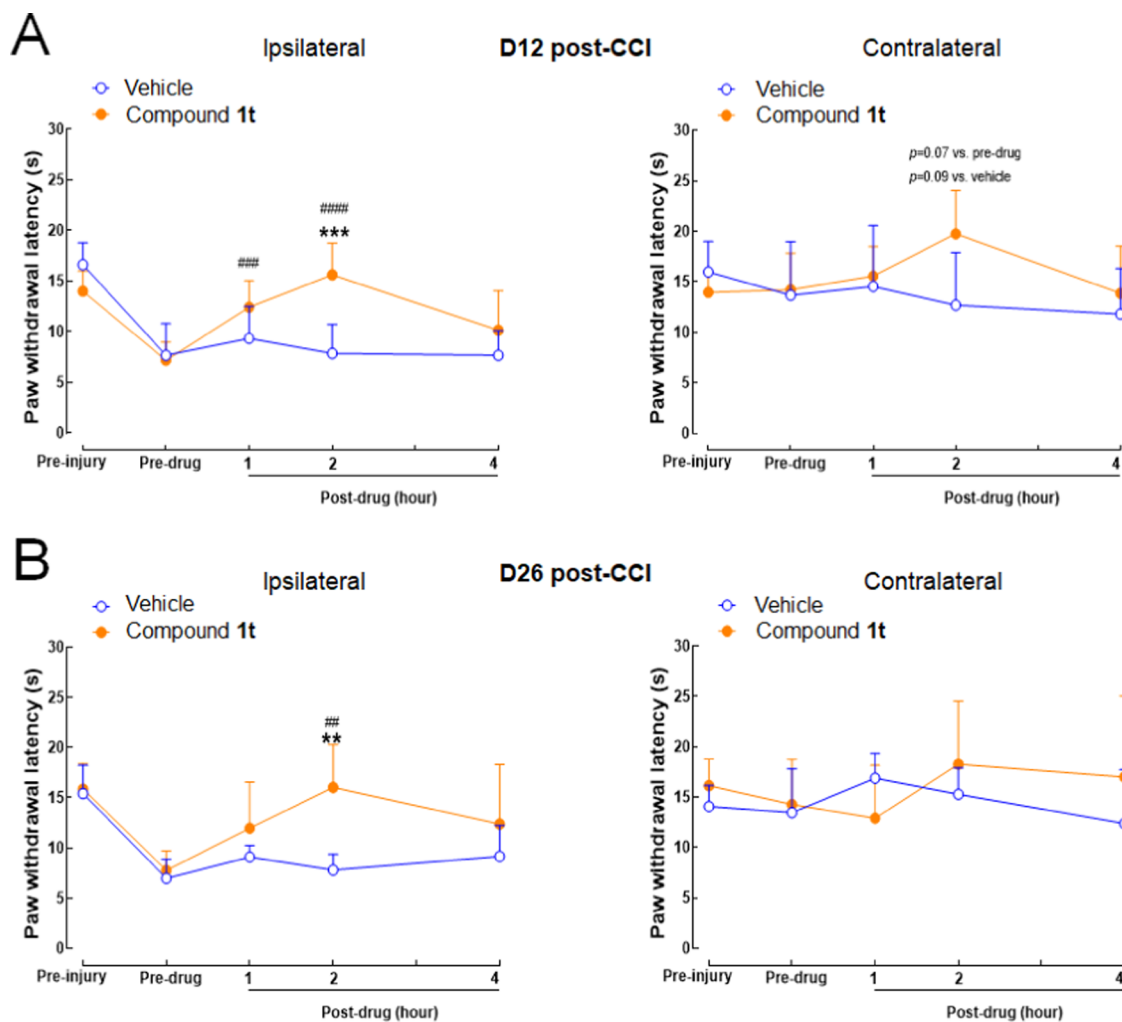


Figure 4. Oral administration of compound **1t** attenuated heat hypersensitivity in the ipsilateral hind paw of MRGPRX1 mice subjected to sciatic nerve CCI. (A) Paw withdrawal latency (PWL) to noxious heat stimuli was measured with the Hargreaves test. PWLs were increased from pre-drug level after being treated with compound **1t** (100 mg/kg, po, $n = 5$), but not those treated with vehicle ($n = 4$) on day 12 post-CCI, and (B) on day 26 post-CCI ($n = 5$ /group). ** $P < 0.01$, *** $P < 0.001$ vs vehicle; ## $P < 0.01$, ### $P < 0.001$, #### $P < 0.0001$ vs pre-drug. Two-way mixed-model analysis of variance (ANOVA) with Bonferroni post hoc test. Data are expressed as mean + standard deviation (SD).

CONCLUSIONS

Chronic pain treatment remains a major medical challenge. There is a critical unmet medical need for new chronic pain therapies devoid of abuse potential and adverse effects. Restricted expression of human MRGPRX1 in primary nociceptive neurons provides a unique opportunity to develop analgesic agents targeting this receptor. The allosteric potentiation of MRGPRX1 appears to be a particularly attractive approach given the preferential upregulation of endogenous MRGPRX1 agonists at the central terminals of primary sensory neurons, eliminating the possibility of itch side effects mediated by peripheral receptors. Using a thieno[2,3-*d*]pyrimidine-based hit compound **1a** identified from our high-throughput screening (HTS) efforts as a molecular template, systematic structural optimization was carried out in an

attempt to improve potency and pharmacokinetic properties. As described in this paper, our iterative efforts led to the discovery of more potent MRGPRX1 PAM **1t** with improved metabolic stability and good oral bioavailability, making it suitable for chronic treatment. As a proof of principle, our results with compound **1t** in a well-established neuropathic pain model represent the first report of *in vivo* efficacy achieved by an orally administered MRGPRX1 modulator in humanized MRGPRX1 mice. Studies are currently underway to not only further characterize compound **1t** as an analgesic agent but also identify more potent MRGPRX1 PAMs using compound **1t** as a new molecular template.

EXPERIMENTAL SECTION

General. All solvents were of reagent grade or high-performance liquid chromatography (HPLC) grade. Unless otherwise noted, all materials were obtained from commercial suppliers and used without further purification. Melting points were obtained on a Mel-Temp apparatus and are uncorrected. ^1H NMR spectra were recorded at 400 or 500 MHz. ^{13}C NMR spectra were recorded at 101 or 125 MHz. The HPLC solvent system consisted of deionized water and acetonitrile, both containing 0.1% formic acid. Preparative HPLC purification was performed on an Agilent 1200 series HPLC system equipped with an Agilent G1315D DAD detector using a Phenomenex Luna 5 μm C18 column (21.2 mm \times 250 mm, 5 μm). Analytical HPLC was performed on an Agilent 1200 series HPLC system equipped with an Agilent G1315D DAD detector (detection at 220 nm) and an Agilent 6120 quadrupole MS detector. Unless otherwise specified, the analytical HPLC conditions involve 20% acetonitrile/80% water for 0.25 min followed by a gradient to 85% acetonitrile/15% water over 1.5 min and continuation of 85% acetonitrile/15% water for 2.25 min with a Luna C18 column (2.1 mm \times 50 mm, 3.5 μm) at a flow rate of 1.25 mL/min. Elemental analysis was performed by Atlantic Microlabs (Norcross, GA). All final compounds biologically tested were confirmed to be of >95% purity by the HPLC methods described above. All animal studies were conducted according to the protocols approved by the Johns Hopkins University Animal Care and Use Committee.

5,6-Dimethyl-4-(*o*-tolylxy)thieno[2,3-*d*]pyrimidine (1a). To a solution of *o*-cresol (0.41 g, 3.78 mmol) in DMF (8 mL) at 0 $^\circ\text{C}$ was added NaH (60% w/w, 0.15 g, 3.78 mmol). After the mixture was stirred at 0 $^\circ\text{C}$ for 10 min, 4-chloro-5,6-dimethylthieno[2,3-*d*]pyrimidine **2a** (0.50 g, 2.52 mmol) was added in one portion as a solid. The reaction was stirred at 0 $^\circ\text{C}$ and was gradually warmed up to rt and stirred overnight. After ice water was added to quench the reaction, the mixture was concentrated and taken up in Et₂O (40 mL). The mixture was washed with H₂O (20 mL) and brine (20 mL), dried over Na₂SO₄, and concentrated. The resulting solid residue was triturated with EtOAc/hexanes (1:4) to afford 0.4 g of the desired product as a white solid (59% yield); mp 106–108 $^\circ\text{C}$. ^1H NMR (CDCl₃) δ 2.20 (s, 3H), 2.53 (s, 3H), 2.59 (s, 3H), 7.15 (dd, J = 1.0 Hz, J = 7.6 Hz, 1H), 7.23 (m, 1H), 7.32 (m, 2H), 8.48 (s, 1H); ^{13}C NMR (CDCl₃) δ 13.6, 13.8, 16.5, 119.9, 122.2, 125.1, 126.0, 127.1, 130.6, 131.4, 132.6, 150.8, 152.2, 163.0, 167.7. LCMS: t_{R} 2.23 min, m/z 271 [M + H]⁺.

4-(*o*-Tolylxy)thieno[2,3-*d*]pyrimidine (1b). Compound **1b** was prepared as described for the preparation of **1a** except 4-chlorothieno[2,3-*d*]pyrimidine **2b** was used in place of 4-chloro-5,6-dimethylthieno[2,3-*d*]pyrimidine **2a**. White solid (82% yield); mp 63–64 $^\circ\text{C}$. ^1H NMR (CDCl₃) δ 2.18 (s, 3H), 7.12–7.39 (m, 4H), 7.49–7.60 (m, 2H), 8.61 (s, 1H); ^{13}C NMR (CDCl₃) δ 16.3, 118.5, 118.9, 122.0, 125.5, 126.3, 127.2, 130.6, 131.5, 150.7, 153.4, 163.4, 169.5. LCMS: t_{R} 1.98 min, m/z 243 [M + H]⁺.

5,6-Dimethyl-4-phenoxythieno[2,3-*d*]pyrimidine (1c). Compound **1c** was prepared as described for the preparation of **1a** except phenol was used in place of *o*-cresol. White solid (67% yield); mp 107–109 $^\circ\text{C}$. ^1H NMR (CDCl₃) δ 2.51 (s, 3H), 2.56 (s, 3H), 7.20–7.33 (m, 3H), 7.44–7.51 (m, 2H), 8.49 (s, 1H); ^{13}C NMR (CDCl₃) δ 13.5, 13.6, 120.1, 121.8, 125.0, 125.6, 129.6, 132.6, 151.9, 152.2, 163.1, 167.7. LCMS: t_{R} 2.16 min, m/z 257 [M + H]⁺.

5,6-Dimethyl-4-(*p*-tolylxy)thieno[2,3-*d*]pyrimidine (1d). Compound **1d** was prepared as described for the preparation of **1a** except *m*-cresol was used in place of *o*-cresol. White solid (44% yield); mp 154–155 $^\circ\text{C}$. ^1H NMR (CDCl₃) δ 2.41 (s, 3H), 2.51 (s, 3H), 2.55 (s, 3H), 6.99–7.07 (m, 2H), 7.11 (d, J = 7.6 Hz, 1H), 7.35 (t, J = 7.7 Hz, 1H), 8.50 (s, 1H); ^{13}C NMR (CDCl₃) δ 13.6, 13.7, 21.4, 118.8, 120.2, 122.4, 125.1, 126.6, 129.4, 132.6, 140.0, 152.1, 152.3, 163.3, 167.8. LCMS: t_{R} 2.29 min, m/z 271 [M + H]⁺.

5,6-Dimethyl-4-(*p*-tolylxy)thieno[2,3-*d*]pyrimidine (1e). Compound **1e** was prepared as described for the preparation of **1a** except *p*-cresol was used in place of *o*-cresol. White powder (50% yield); mp 90–94 $^\circ\text{C}$. ^1H NMR (CDCl₃) δ 2.40 (s, 3H), 2.50 (s, 3H), 2.56 (s,

3H), 7.11 (d, J = 8.4 Hz, 2H), 7.26 (d, J = 8.4 Hz, 2H), 8.49 (s, 1H); ^{13}C NMR (CDCl₃) δ 13.5, 13.6, 20.9, 120.1, 121.50, 121.52, 125.1, 130.19, 130.21, 132.5, 135.3, 150.0, 152.01, 152.03, 163.4, 167.6. LCMS: t_{R} 2.26 min, m/z 271 [M + H]⁺.

4-(2-Fluorophenoxy)-5,6-dimethylthieno[2,3-*d*]pyrimidine (1f). Compound **1f** was prepared as described for the preparation of **1a** except 2-fluorophenol was used in place of *o*-cresol. White powder (75% yield); mp 143–145 $^\circ\text{C}$. ^1H NMR (CDCl₃) δ 2.53 (s, 3H), 2.59 (s, 3H), 7.22–7.39 (m, 4H), 8.50 (s, 1H); ^{13}C NMR (CDCl₃) δ 13.57, 13.62, 116.8 (d, J_{CF} = 18.3 Hz), 119.8, 124.0, 124.6 (d, J_{CF} = 4 Hz), 125.0, 127.0 (d, J_{CF} = 7 Hz), 133.0, 139.6 (d, J_{CF} = 12.7 Hz), 151.77, 151.82, 154.5 (d, J_{CF} = 249 Hz), 162.3, 167.9. LCMS: t_{R} 2.22 min, m/z 275 [M + H]⁺.

4-(3-Fluorophenoxy)-5,6-dimethylthieno[2,3-*d*]pyrimidine (1g). Compound **1g** was prepared as described for the preparation of **1a** except 3-fluorophenol was used in place of *o*-cresol. White solid (62% yield); mp 158–161 $^\circ\text{C}$. ^1H NMR (CDCl₃) δ 2.51 (s, 3H), 2.53–2.56 (m, 5H), 6.96–7.07 (m, 5H), 7.38–7.47 (m, 1H), 8.50 (s, 1H); ^{13}C NMR (CDCl₃) δ 13.6, 109.9 (d, J_{CF} = 24.2 Hz), 112.7 (d, J_{CF} = 20.9 Hz), 117.6 (d, J_{CF} = 3.4 Hz), 120.1, 124.9, 130.4 (d, J_{CF} = 9.3 Hz), 133.2, 151.8, 153.2 (d, J_{CF} = 10.8 Hz), 162.6, 163.1 (d, J_{CF} = 248 Hz), 168.0. LCMS: t_{R} 2.16 min, m/z 275 [M + H]⁺.

4-(4-Fluorophenoxy)-5,6-dimethylthieno[2,3-*d*]pyrimidine (1h). Compound **1h** was prepared as described for the preparation of **1a** except 4-fluorophenol was used in place of *o*-cresol. White fluffy needles (54% yield); mp 137–140 $^\circ\text{C}$. ^1H NMR (CDCl₃) δ 2.51 (s, 3H), 2.55 (s, 3H), 7.12–7.22 (m, 5H), 8.48 (s, 1H); ^{13}C NMR (CDCl₃) δ 13.6, 13.7, 116.3 (d, J_{CF} = 23.6 Hz), 120.0, 123.3 (d, J_{CF} = 8.3 Hz), 125.0, 132.9, 148.0 (d, J_{CF} = 3 Hz), 151.8, 160.1 (d, J_{CF} = 244 Hz), 163.1, 167.8. LCMS: t_{R} 2.16 min, m/z 275 [M + H]⁺.

5,6-Dimethyl-4-(2-(trifluoromethyl)phenoxy)thieno[2,3-*d*]pyrimidine (1i). Compound **1i** was prepared as described for the preparation of **1a** except 2-(trifluoromethyl)phenol was used in place of *o*-cresol. White powder (53% yield). mp 155–157 $^\circ\text{C}$. ^1H NMR (CDCl₃) δ 2.52 (s, 3H), 2.55 (s, 3H), 7.34–7.45 (m, 2H), 7.64–7.70 (m, 1H), 7.77 (d, J = 7.9 Hz, 1H), 8.47 (s, 1H). ^{13}C NMR (CDCl₃) δ 13.3, 13.7, 120.0, 123.0 (q, J_{CF} = 273 Hz), 123.4, 124.7, 125.1, 125.7, 127.2 (q, J_{CF} = 4.8 Hz), 133.0, 133.2, 149.65, 151.6, 162.5, 168.1. LCMS: t_{R} 2.29 min, m/z 325 [M + H]⁺.

5,6-Dimethyl-4-(3-(trifluoromethyl)phenoxy)thieno[2,3-*d*]pyrimidine (1j). Compound **1j** was prepared as described for the preparation of **1a** except 3-(trifluoromethyl)phenol was used in place of *o*-cresol. White solid (71% yield); mp 120–126 $^\circ\text{C}$. ^1H NMR (CDCl₃) δ 2.52 (s, 3H), 2.56 (s, 3H), 7.40–7.65 (m, 4H), 8.49 (s, 1H); ^{13}C NMR (CDCl₃) δ 13.6, 119.1 (q, J_{CF} = 3.8 Hz), 120.1, 122.4 (q, J_{CF} = 3.9 Hz), 123.5 (q, J_{CF} = 272 Hz), 124.8, 125.5, 130.1, 132.1 (q, J_{CF} = 32.9 Hz), 133.3, 151.6, 152.4, 162.5, 168.1. LCMS: t_{R} 2.38 min, m/z 325 [M + H]⁺.

5,6-Dimethyl-4-(4-(trifluoromethyl)phenoxy)thieno[2,3-*d*]pyrimidine (1k). Compound **1k** was prepared as described for the preparation of **1a** except 4-(trifluoromethyl)phenol was used in place of *o*-cresol. Light yellow needles (33% yield); mp 115–120 $^\circ\text{C}$. ^1H NMR (CDCl₃) δ 2.52 (s, 3H), 2.55 (s, 3H), 7.36 (d, 2H), 7.73 (d, 2H), 8.49 (s, 1H). ^{13}C NMR (CDCl₃) δ 13.62, 13.65, 120.2, 122.2, 123.9 (q, J_{CF} = 271 Hz), 124.8, 127.0 (q, J_{CF} = 3.7 Hz), 127.8 (q, J_{CF} = 32.9 Hz), 133.4, 151.66, 151.70, 154.9, 162.4, 168.2. LCMS: t_{R} 2.35 min, m/z 325 [M + H]⁺.

4-(2-Fluorophenoxy)thieno[2,3-*d*]pyrimidine (1l). Compound **1l** was prepared as described for the preparation of **1a** except 2-fluorophenol was used in place of *o*-cresol and 4-chlorothieno[2,3-*d*]pyrimidine **2b** was used in place of 4-chloro-5,6-dimethylthieno[2,3-*d*]pyrimidine **2a**. White solid (36% yield); mp 104–106 $^\circ\text{C}$. ^1H NMR (CDCl₃) δ 7.20–7.37 (m, 4H), 7.53 (d, J = 5.9 Hz, 1H), 7.57 (dd, J = 6.0, 0.6 Hz, 1H), 8.62 (s, 1H). ^{13}C NMR (CDCl₃) δ 116.9 (d, J_{CF} = 18.3 Hz), 117.0, 118.4, 118.7, 123.9, 124.8 (d, J_{CF} = 3.7 Hz), 125.9, 127.2 (d, J_{CF} = 7.1 Hz), 139.4 (d, J_{CF} = 12.6 Hz), 153.1, 154.4 (d, J_{CF} = 250 Hz), 162.8, 169.7. LCMS: t_{R} 1.92 min, m/z 247 [M + H]⁺.

4-(2-Fluorophenoxy)-5-methylthieno[2,3-*d*]pyrimidine (1m). Compound **1m** was prepared as described for the preparation of **1a**

except 2-fluorophenol was used in place of *o*-cresol and 4-chloro-5-methylthieno[2,3-*d*]pyrimidine **2c** was used in place of 4-chloro-5,6-dimethylthieno[2,3-*d*]pyrimidine **2a**. Beige fluffy solid (93% yield); mp 98–102 °C. ¹H NMR (CDCl₃) δ 2.69 (s, 3H), 7.09 (s, 1H), 7.19–7.38 (m, 4H), 8.55 (s, 1H). ¹³C NMR (CDCl₃) δ 17.0, 116.9 (d, *J*_{CF} = 18.3 Hz), 118.6, 120.6, 124.0, 124.7 (d, *J*_{CF} = 3.9 Hz), 127.1 (d, *J*_{CF} = 6.9 Hz), 130.5, 139.5 (d, *J*_{CF} = 12.6 Hz), 152.9, 154.5 (d, *J*_{CF} = 249 Hz), 163.6, 170.4. LCMS: *t*_R 2.07 min, *m/z* 261 [M + H]⁺.

4-(2-Fluorophenoxy)-6-methylthieno[2,3-*d*]pyrimidine (1n). Compound **1n** was prepared as described for the preparation of **1a** except 2-fluorophenol was used in place of *o*-cresol and 4-chloro-6-methylthieno[2,3-*d*]pyrimidine **2d** was used in place of 4-chloro-5,6-dimethylthieno[2,3-*d*]pyrimidine **2a**. White solid (84% yield); mp 135–138 °C. ¹H NMR (CDCl₃) δ 2.67 (s, 3H), 7.19–7.37 (m, 5H), 8.55 (s, 1H). ¹³C NMR (CDCl₃) δ 16.4, 115.5, 116.9 (d, *J*_{CF} = 18.5 Hz), 119.5, 123.9, 124.7 (d, *J*_{CF} = 3.9 Hz), 127.1 (d, *J*_{CF} = 7 Hz), 139.5 (d, *J*_{CF} = 12.5 Hz), 140.8, 152.2, 154.4 (d, *J*_{CF} = 250 Hz), 161.5, 169.5. LCMS: *t*_R 2.07 min, *m/z* 261 [M + H]⁺.

4-(2-Fluorophenoxy)-5-(trifluoromethyl)thieno[2,3-*d*]pyrimidine (1o). Compound **1o** was prepared as described for the preparation of **1a** except 2-fluorophenol was used in place of *o*-cresol and 4-chloro-5-(trifluoromethyl)thieno[2,3-*d*]pyrimidine **2e**¹⁶ was used in place of 4-chloro-5,6-dimethylthieno[2,3-*d*]pyrimidine **2a**. White cake solid (90% yield); mp 65–66 °C. ¹H NMR (CDCl₃) δ 7.22–7.27 (m, 2H), 7.28–7.34 (m, 2H), 8.03 (s, 1H), 8.67 (s, 1H). ¹³C NMR (CDCl₃) δ 114.4, 117.0 (d, *J*_{CF} = 18.2 Hz), 121.1 (q, *J*_{CF} = 270 Hz), 123.2 (q, *J*_{CF} = 38 Hz), 123.7, 124.8 (d, *J*_{CF} = 4.1 Hz), 127.5 (d, *J*_{CF} = 7 Hz), 128.4 (q, *J*_{CF} = 5.9 Hz), 139.2 (d, *J*_{CF} = 12.7 Hz), 154.2, 154.3 (d, *J*_{CF} = 250 Hz), 162.3, 170.3. LCMS: *t*_R 2.13 min, *m/z* 315 [M + H]⁺.

6-(tert-Butyl)-4-(2-fluorophenoxy)thieno[2,3-*d*]pyrimidine (1p). Compound **1p** was prepared as described for the preparation of **1a** except 2-fluorophenol was used in place of *o*-cresol and 6-(tert-butyl)-4-chlorothieno[2,3-*d*]pyrimidine **2f** was used in place of 4-chloro-5,6-dimethylthieno[2,3-*d*]pyrimidine **2a**. Clear oil (60% yield). ¹H NMR (CDCl₃) δ 1.51 (s, 9H), 7.21–7.35 (m, 5H), 8.54 (s, 1H). ¹³C NMR (CDCl₃) δ 32.0, 35.4, 111.7, 116.9 (d, *J*_{CF} = 18.3 Hz), 119.1, 123.9, 124.8 (d, *J*_{CF} = 3.8 Hz), 127.1 (d, *J*_{CF} = 7.2 Hz), 139.6 (d, *J*_{CF} = 12.6 Hz), 152.3, 154.5 (d, *J*_{CF} = 250 Hz), 158.1, 161.8, 169.0. LCMS: *t*_R 2.41 min, *m/z* 303 [M + H]⁺.

6-tert-Butyl-5-phenylthieno[2,3-*d*]pyrimidin-4-ol (4). In a vial, 3,3-dimethyl-1-phenylbutan-1-one **3** (500 mg, 2.84 mmol), ethylcyanoacetate (483 mg, 4.26 mmol), sulfur (726 mg, 2.84 mmol), formamide (0.9 mL, 22.7 mmol), *L*-proline (65.3 mg, 0.57 mmol), and diethylamine (41.5 mg, 0.57 mmol) were heated to 170 °C and stirred for 6 h. After the vial was cooled to rt, the residue was triturated with DCM. The resulting black solid was removed by filtration, and the filtrate was concentrated and purified by Biotage Isolera One using 30–50% EtOAc in DCM as an eluent to give 35 mg of the desired compound as a yellow solid (4% yield). ¹H NMR (CDCl₃) δ 1.24 (s, 9H), 7.25–7.31 (m, 2H), 7.34–7.46 (m, 3H), 10.91 (s, 1H). LCMS: *t*_R 1.98 min, *m/z* 285 [M + H]⁺.

6-tert-Butyl-4-chloro-5-phenylthieno[2,3-*d*]pyrimidine (5). A solution of **4** (35 mg, 0.12 mmol) in POCl₃ (0.5 mL) was stirred at 110 °C for 1 h. Excess POCl₃ was removed in vacuo followed by co-evaporation with DCM three times. The crude was purified by Biotage Isolera One using 0–10% EtOAc in DCM as an eluent to give 25 mg of the desired compound as a yellow oil (66% yield). ¹H NMR (CDCl₃) δ 1.30 (s, 9H), 7.28–7.32 (m, 2H), 7.38–7.47 (m, 3H), 8.76 (s, 1H). LCMS: *t*_R 2.44 min, *m/z* 303 [M + H]⁺.

6-tert-Butyl-4-(2-fluorophenoxy)-5-phenylthieno[2,3-*d*]pyrimidine (1q). Sodium hydride (60% dispersion in mineral oil, 5.3 mg, 0.13 mmol) in DMF (0.2 mL) at 0 °C, and the mixture was stirred at 0 °C for 5–10 min. A solution of **5** (20 mg, 0.07 mmol) in DMF (0.3 mL) was then added slowly to the mixture via a syringe at 0 °C. The reaction mixture was stirred and allowed to warm to rt overnight. A few drops of 10% KHSO₄ were added to the mixture to quench the excess NaH, and the mixture was then concentrated in vacuo. The crude residue was triturated in methanol and water to give 10 mg of

the desired compound as a light yellow solid (40% yield); mp 81–82 °C. ¹H NMR (CDCl₃) δ 1.33 (s, 9H), 6.92 (dt, *J* = 8.4, 4.1 Hz, 1H), 7.03–7.17 (m, 3H), 7.27–7.44 (m, 5H), 8.50 (s, 1H); ¹³C NMR (CDCl₃) δ 32.6, 36.4, 116.6 (d, *J*_{CF} = 18 Hz), 123.5, 124.4, 126.6 (d, *J*_{CF} = 7 Hz), 127.4, 127.5, 129.1, 130.4, 137.1, 143.0 (d, *J*_{CF} = 19 Hz), 151.0, 152.2, 154.1 (d, *J*_{CF} = 250 Hz), 162.2, 165.9. LCMS: *t*_R 2.64 min, *m/z* 379 [M + H]⁺.

6-tert-Butyl-4-methoxythieno[2,3-*d*]pyrimidine (6). To a solution of 6-tert-butyl-4-chlorothieno[2,3-*d*]pyrimidine **2f** (1.62 g, 7.15 mmol) in methanol (20 mL) at 0 °C was added 25 wt % sodium methoxide in methanol (17.2 mmol, 3.92 mL). The mixture was stirred at 0 °C for 30 min, then at rt for 1 h. The solvent was removed in vacuo, and water was carefully added to quench excess sodium methoxide. The compound was extracted with EtOAc, and the organic layer was dried over Na₂SO₄ and concentrated to give 1.56 g of the desired compound as a yellow oil, which was used without further purification (98% crude yield). ¹H NMR (CDCl₃) δ 1.45 (s, 9H), 4.12 (s, 3H), 7.06 (s, 1H), 8.59 (s, 1H).

5-Bromo-6-tert-butyl-4-methoxythieno[2,3-*d*]pyrimidine (7). To a solution of **6** (1.56 g, 7.02 mmol) in AcOH (30 mL) was added *N*-bromosuccinimide (3.75 g, 21.1 mmol), and the mixture was stirred at 55 °C overnight. The reaction was concentrated, and the crude material was purified by Biotage Isolera One using 0–10% EtOAc in hexanes as an eluent to give 1.8 g of the desired compound as a light yellow solid (85% yield). ¹H NMR (CDCl₃) δ 1.59 (s, 9H), 4.14 (s, 3H), 8.59 (s, 1H).

6-(tert-Butyl)-5-(4-fluorophenyl)-4-methoxythieno[2,3-*d*]pyrimidine (8a). A suspension of **7** (200 mg, 0.66 mmol), 4-fluorophenylboronic acid (186 mg, 1.33 mmol), potassium carbonate (4.13 g, 29.9 mmol), and bis(triphenylphosphine)palladium(II) dichloride (46.6 mg, 0.07 mmol) in DMF (8 mL) was purged with N₂ gas via an inserted long needle for 30 min. The mixture was then stirred at 80 °C overnight. After removing the solvent in vacuo, water was added to the mixture. The mixture was extracted with dichloromethane twice and the combined extracts were washed with brine, dried over Na₂SO₄, and concentrated. The resulting white precipitate was removed by filtration, and the filtrate was concentrated and purified by Biotage Isolera One using 5% EtOAc/DCM as an eluent to give 190 mg of the desired compound as a thick brown oil (92% yield). ¹H NMR (CDCl₃) δ 1.27 (s, 9H), 3.69 (s, 3H), 7.02–7.12 (m, 2H), 7.19–7.26 (m, 2H), 8.56 (s, 1H).

6-tert-Butyl-5-(3,4-dichlorophenyl)-4-methoxythieno[2,3-*d*]pyrimidine (8b). A suspension of **7** (3.00 g, 9.96 mmol), 3,4-dichlorophenylboronic acid (3.80 g, 19.9 mmol), potassium carbonate (4.13 g, 29.9 mmol), and bis(triphenylphosphine)palladium(II) dichloride (0.699 g, 1.00 mmol) in DMF (45 mL) was purged with N₂ gas via an inserted long needle for 30 min. The mixture was then stirred at 80 °C overnight. After removing the solvent in vacuo, water was added to the mixture. The mixture was extracted with dichloromethane twice and the combined extracts were washed with brine, dried over Na₂SO₄, and concentrated. The resulting white precipitate was removed by filtration, and the filtrate was concentrated and purified by Biotage Isolera One using 5% EtOAc/DCM as an eluent to give 2.73 g of the desired compound as a thick brown oil (75% yield). ¹H NMR (CDCl₃) δ 1.30 (s, 9H), 3.74 (s, 3H), 7.13 (dd, *J* = 2.0, 8.1 Hz, 1H), 7.40 (d, *J* = 2.0 Hz, 1H), 7.45 (d, *J* = 8.3 Hz, 1H), 8.58 (s, 1H).

6-tert-Butyl-5-(4-fluorophenyl)thieno[2,3-*d*]pyrimidin-4-ol (9a). To a solution of **8a** (189 mg, 0.60 mmol) in DCM (6 mL) at 0 °C was added 1 M BBr₃ solution in DCM (1.80 mL, 1.80 mmol). The mixture was stirred at 0 °C, then gradually warmed to rt, and stirred until completion (overnight). The mixture was then cooled to 0 °C, and methanol was added to quench excess BBr₃. After the removal of solvents, the crude material was partitioned between water and dichloromethane. The organic layer was washed with brine, dried over Na₂SO₄, and concentrated. The residual solid was purified by Biotage Isolera One using 20–35% EtOAc in hexanes with 2% AcOH as an eluent to give 75 mg of the desired compound as a white solid (41% yield). ¹H NMR (CDCl₃) δ 1.25 (s, 9H), 7.05–7.12 (m, 2H), 7.22–7.27 (m, 2H), 7.77 (s, 1H), 10.59 (s, 1H).

6-tert-Butyl-5-(3,4-dichlorophenyl)thieno[2,3-d]pyrimidin-4-ol (9b). To a solution of **8b** (1.50 g, 4.08 mmol) in DCM (50 mL) at 0 °C was added 1 M BBr₃ solution in DCM (20.4 mL, 20.4 mmol). The mixture was stirred at 0 °C, then gradually warmed to rt, and stirred until completion (7 days). The mixture was then cooled to 0 °C, and methanol was added to quench excess BBr₃. After the removal of solvents, the crude material was partitioned between water and dichloromethane. The organic layer was washed with brine, dried over Na₂SO₄, and concentrated. The residual solid was triturated with dichloromethane to give 1.27 g of the desired compound as a white solid (93% yield). ¹H NMR (CDCl₃) δ 1.28 (s, 9H), 7.14 (dd, *J* = 2.0, 8.1 Hz, 1H), 7.40 (d, *J* = 2.0 Hz, 1H), 7.46 (d, *J* = 8.3 Hz, 1H), 7.76 (s, 1H), 11.25 (s, 1H).

6-tert-Butyl-4-chloro-5-(4-fluorophenyl)thieno[2,3-d]pyrimidine (10a). A solution of **9a** (70 mg, 0.23 mmol) in POCl₃ (3 mL) was stirred at 110 °C for 1 h. Excess POCl₃ was removed in vacuo followed by co-evaporation with DCM (three times). The residual material was passed through a short silica column using 5% EtOAc in hexanes as an eluent to give 45 mg of the desired compound as a yellow solid (61% yield). ¹H NMR (CDCl₃) δ 1.30 (s, 9H), 7.08–7.18 (m, 2H), 7.24–7.34 (m, 2H), 8.77 (s, 1H).

6-tert-Butyl-4-chloro-5-(3,4-dichlorophenyl)thieno[2,3-d]pyrimidine (10b). A solution of **9b** (2.00 g, 5.66 mmol) in POCl₃ (15 mL) was stirred at 110 °C for 1 h. Excess POCl₃ was removed in vacuo followed by co-evaporation with DCM (three times). The residual material was passed through a short silica column using 0–10% EtOAc in DCM as an eluent to give 2.00 g of the desired compound as a white solid (95% yield). ¹H NMR (CDCl₃) δ 1.33 (s, 9H), 7.17 (dd, *J* = 2.0, 8.3 Hz, 1H), 7.45 (d, *J* = 2.0 Hz, 1H), 7.51 (d, *J* = 8.1 Hz, 1H), 7.79 (s, 1H).

6-(tert-Butyl)-4-(2-fluorophenoxy)-5-(4-fluorophenyl)thieno[2,3-d]pyrimidine (1r). To a solution of 2-fluorophenol (41.9 mg, 0.37 mmol) in DMF (1 mL) was added sodium hydride (60% dispersion in mineral oil, 11.2 mg, 0.28 mmol) at 0 °C, and the mixture was stirred at 0 °C for 5–10 min. A solution of **10a** (60 mg, 0.19 mmol) in DMF (2 mL) was then slowly added to the mixture via a syringe at 0 °C. The reaction mixture was gradually warmed up to rt and stirred overnight. A few drops of 10% KHSO₄ was added to the mixture to quench excess NaH, and the mixture was concentrated in vacuo. The crude material was partitioned between water and EtOAc. The organic layer was washed with brine, dried over sodium sulfate, and concentrated. The residual material was purified by Biotage Isolera One using 10% EtOAc in hexanes as an eluent to give 60 mg of the desired compound as a light tan solid (77% yield); mp 172–173 °C. ¹H NMR (CDCl₃) δ 1.33 (s, 9H), 6.94 (t, *J* = 8.0 Hz, 1H), 7.01–7.22 (m, 5H), 7.32–7.43 (m, 2H), 8.51 (s, 1H); ¹³C NMR (CDCl₃) δ 32.6, 36.4, 114.5 (d, *J*_{CF} = 21 Hz), 116.7 (d, *J*_{CF} = 18 Hz), 120.4, 123.6, 124.4 (d, *J*_{CF} = 4 Hz), 126.7 (d, *J*_{CF} = 6.8 Hz), 127.9, 132.0 (d, *J*_{CF} = 8.1 Hz), 133.0 (d, *J*_{CF} = 3.5 Hz), 139.3 (d, *J*_{CF} = 12.7 Hz), 151.6, 152.4, 154.1 (d, *J*_{CF} = 249 Hz), 162.2, 162.3 (d, *J*_{CF} = 247 Hz), 165.9. LCMS: *t*_R 2.63 min, *m/z* 397 [M + H]⁺.

6-(tert-Butyl)-5-(4-fluorophenyl)-4-(2-(trifluoromethoxy)phenoxy)thieno[2,3-d]pyrimidine (1s). To a solution of 2-trifluoromethoxyphenol (35 mg, 0.31 mmol) in DMF (1 mL) was added sodium hydride (60% dispersion in mineral oil, 12.5 mg, 0.31 mmol) at 0 °C, and the mixture was stirred at 0 °C for 5–10 min. A solution of **10b** (50 mg, 0.16 mmol) in DMF (1 mL) was then slowly added to the mixture via a syringe at 0 °C. The reaction mixture was gradually warmed up to rt and stirred overnight. A few drops of 10% KHSO₄ were added to the mixture to quench excess NaH, and the mixture was concentrated in vacuo. The crude material was partitioned between water and EtOAc. The organic layer was washed with brine, dried over sodium sulfate, and concentrated. The residual material was purified by Biotage Isolera One using 0–10% EtOAc in hexanes as an eluent to give 46 mg of the desired compound as a yellow solid (65% yield); mp 127–129 °C. ¹H NMR (CDCl₃) δ 1.33 (s, 9H), 6.98–7.07 (m, 3H), 7.22–7.38 (m, 5H), 8.49 (s, 1H); ¹³C NMR (CDCl₃) δ 29.6, 32.5, 36.4, 114.5 (d, *J*_{CF} = 21.5 Hz), 120.2 (q, *J*_{CF} = 259 Hz), 120.3, 122.3, 122.7, 124.0, 124.4, 126.5, 126.8, 127.6, 127.8, 127.9, 132.0 (d, *J*_{CF} = 8.1 Hz), 132.8 (d, *J*_{CF} = 3.7 Hz), 140.87,

140.90, 143.8, 151.7, 152.2, 152.4, 162.2, 162.3 (d, *J*_{CF} = 246 Hz), 165.9. LCMS: *t*_R 2.63 min, *m/z* 463 [M + H]⁺.

6-tert-Butyl-5-(3,4-dichlorophenyl)-4-(2-(trifluoromethoxy)phenoxy)thieno[2,3-d]pyrimidine (1t). To a solution of 2-trifluoromethoxyphenol (0.529 g, 2.97 mmol) in DMF (6 mL) was added sodium hydride (60% dispersion in mineral oil, 0.119 g, 2.97 mmol) at 0 °C, and the mixture was stirred at 0 °C for 5–10 min. A solution of **10b** (0.920 g, 2.48 mmol) in DMF (15 mL) was then slowly added to the mixture via a syringe at 0 °C. The reaction mixture was gradually warmed up to rt and stirred overnight. A few drops of 10% KHSO₄ were added to the mixture to quench excess NaH, and the mixture was concentrated in vacuo. The crude material was partitioned between water and EtOAc. The organic layer was washed with brine, dried over sodium sulfate, and concentrated. The residual material was purified by Biotage Isolera One using CHCl₃ as an eluent to give 0.880 g of the desired compound as a white solid (69% yield); mp 85–89 °C. ¹H NMR (CDCl₃) δ 1.35 (s, 9H), 7.02 (m, 1H), 7.23–7.33 (m, 4H), 7.43 (d, *J* = 8.3 Hz, 1H), 7.51 (d, *J* = 2.0 Hz, 1H), 8.51 (s, 1H); ¹³C NMR (CDCl₃) δ 32.6, 36.5, 119.9, 120.2 (q, *J*_{CF} = 259 Hz), 122.4, 124.1, 126.2, 126.7, 127.7, 129.5, 129.9, 131.6, 131.8, 132.2, 137.0, 140.9, 143.7, 152.3, 152.4, 162.1, 166.0. LCMS: *t*_R 2.98 min, *m/z* 513.1 [M + H]⁺. Anal. calcd for C₂₃H₁₇Cl₂F₃N₂O₂S: C, 53.81; H, 3.34; N, 5.46; S, 6.25; F, 11.10; Cl, 13.81. Found: C, 53.82; H, 3.41; N, 5.38, S, 6.23; F, 10.93; Cl, 13.87.

In Vitro MRGPRX1 Receptor Assay. HEK293 cells stably transfected with human *MrgprX1* were plated in 96-well plates at 25 000 cell/well and incubated 2 days before imaging. On the day of imaging, the cells were incubated in 100 μL of Hanks' Balanced Salt Solution (HBSS) with 2 μM Fluo 4AM and 1% Trypan Red for 50 min at 37 °C. The cells were then equilibrated for 10 min at room temperature before imaging. Test compounds were dissolved in HBSS and underwent a serial dilution. Test compounds, BAM 8–22 (positive control) or HBSS (negative control) were added (50 μL into 100 μL), and the cells were imaged on the FLIPR for 2 min. Data were exported as maximum–minimum fluorescent signal.

In Vitro Metabolic Stability Studies. The metabolic stability was evaluated using mouse and human liver microsomes as previously reported.¹⁷ The assay was carried out with 100 mM potassium phosphate buffer, pH 7.4, in the presence of NADPH regenerating system (1.3 mM NADPH, 3.3 mM glucose-6-phosphate, 3.3 mM MgCl₂, 0.4 U/mL glucose-6-phosphate dehydrogenase, 50 μM sodium citrate). Reactions, in triplicate, were initiated by the addition of liver microsomes to the incubation mixture (compound final concentration was 5 μM; 0.5 mg/mL microsomes). Controls in the absence of cofactors were carried out to determine the specific cofactor-free degradation. After 30 and 60 min of incubation, aliquots of the mixture were removed in triplicate and the reaction was quenched by the addition of three times the volume of ice-cold acetonitrile spiked with the internal standard. Compound disappearance was monitored over time using a liquid chromatography and tandem mass spectrometry (LC–MS/MS) method.

Metabolite Identification Studies. Metabolite identification was performed on samples obtained from human liver microsomes. Samples (2 μL) were injected on an Agilent 1290 UPLC coupled to an Agilent 6520 quadrupole time-of-flight mass spectrometer. Metabolites were separated on an Agilent Eclipse Plus C18 1.8 μm, 2.1 mm × 100 mm column with a 5 min gradient from 97.5/2.5 to 5/95 water + 0.1% formic acid/acetonitrile + 0.1% formic acid mobile phase. Analysis was performed in positive-ion mode, with fragmentation by collision-induced dissociation with a collision energy of 25. Product ions were identified using MassHunter Qualitative analysis software.

In Vivo Pharmacokinetic Studies in Mice. All pharmacokinetic studies in mice were conducted according to protocols approved by the Animal Care and Use Committee at Johns Hopkins University. Male CD 1 mice between 25 and 30 g were obtained from Harlan, Inc. and maintained on a 12 h light–dark cycle with *ad libitum* access to food and water. Compound **1t** was given to the mice (*n* = 3) by oral gavage at 100 mg/kg in a vehicle (5% dimethyl acetamide, 10% Cremophor EL, 10% Tween 80, 25% PEG400, and 50% water). The

mice were sacrificed at predetermined time points (0.25–6 h) post drug administration. For the collection of plasma and spinal cord and brain, the animals were euthanized with CO₂ and blood samples were collected in heparinized microtubes by cardiac puncture. Spinal cords and brains were dissected and immediately flash-frozen (–80 °C). Plasma was obtained by centrifugation of blood at 3000g for 15 min and stored at –80 °C until LC–MS analysis.

Prior to extraction, frozen samples were thawed on ice. The calibration curves were developed using plasma and spinal cord from naïve animals as a matrix. Plasma samples (50 µL) were processed using a single liquid extraction method by the addition of 300 µL of acetonitrile as with internal standard (losartan [5 µM]), followed by vortexing for 30 s and then centrifugation at 10 000 rcf for 10 min. For spinal cord tissue, homogenized samples were vortexed and centrifuged as above. A 10 µL aliquot of the supernatant was diluted with 40 µL of water containing 0.5 µM losartan as internal standard. Extracts were centrifuged at 10 000 rcf at 4 °C for 10 min. Supernatants were transferred to 250 µL polypropylene autosampler vials sealed with a Teflon cap. A volume of 3 µL was injected onto the ultraperformance liquid chromatography (UPLC) instrument for quantitative analysis by LC–MS/MS. Calibration curves over the 0.01–10 nmol/mL plasma and spinal cord were constructed from the peak area ratio of the analyte to the internal standard using linear regression with a weighting factor of 1/(nominal concentration). A correlation coefficient greater than 0.99 was obtained in all analytical runs for all analytes.

Sciatic Nerve Chronic Constrictive Injury (CCI) Model of Neuropathic Pain. MRGPRX1 mice were generated as described in our previous study.⁸ MRGPRX1 mice (both sexes) were bred at the Johns Hopkins University and had access *ad libitum* to food and water. Neuropathic pain was induced by CCI surgery to the sciatic nerve in adult mice (2- to 3-month-old, 20–30 g). The mice were anesthetized by the inhalation of 2% isoflurane delivered through a nose cone. The skin was shaved, and a small incision was made at the level of the mid-thigh. The left sciatic nerve was exposed by blunt dissection through the biceps femoris and separated from the surrounding tissue. The nerve trunk proximal to the distal branching point was loosely tied with three nylon sutures (6–0 nonabsorbable braided silk suture, 18020-60, Fine Science Tools, CA) until the epineurium was slightly compressed and minor twitching of the relevant muscles was observed. The ligatures were approximately 0.5 mm apart. The muscle layer was closed with 4-0 silk suture, and the wound was closed with suture.

■ ASSOCIATED CONTENT

SI Supporting Information

The Supporting Information is available free of charge at <https://pubs.acs.org/doi/10.1021/acs.jmedchem.1c01709>.

¹H and ¹³C spectra of the final compounds, *in vitro* selectivity profile of compound **1t**, and behavioral effects of compound **1t** in naïve MRGPRX1 mice (PDF)

Molecular formula strings (CSV)

■ AUTHOR INFORMATION

Corresponding Authors

Rana Rais – Johns Hopkins Drug Discovery and Department of Neurology, Johns Hopkins University, Baltimore, Maryland 21205, United States; orcid.org/0000-0003-4059-2453; Email: rrais2@jhmi.edu

Takashi Tsukamoto – Johns Hopkins Drug Discovery and Department of Neurology, Johns Hopkins University, Baltimore, Maryland 21205, United States; orcid.org/0000-0002-0216-7520; Email: ttsukamoto@jhmi.edu

Authors

- Ilyas Berhane** – Johns Hopkins Drug Discovery and Department of Neurology, Johns Hopkins University, Baltimore, Maryland 21205, United States
- Niyada Hin** – Johns Hopkins Drug Discovery, Johns Hopkins University, Baltimore, Maryland 21205, United States
- Ajit G. Thomas** – Johns Hopkins Drug Discovery, Johns Hopkins University, Baltimore, Maryland 21205, United States
- Qian Huang** – Department of Anesthesiology and Critical Care Medicine, Johns Hopkins University, Baltimore, Maryland 21205, United States; orcid.org/0000-0001-6039-103X
- Chi Zhang** – Department of Anesthesiology and Critical Care Medicine, Johns Hopkins University, Baltimore, Maryland 21205, United States
- Vijayabhaskar Veeravalli** – Johns Hopkins Drug Discovery and Department of Neurology, Johns Hopkins University, Baltimore, Maryland 21205, United States
- Ying Wu** – Johns Hopkins Drug Discovery, Johns Hopkins University, Baltimore, Maryland 21205, United States
- Justin Ng** – Johns Hopkins Drug Discovery, Johns Hopkins University, Baltimore, Maryland 21205, United States
- Jesse Alt** – Johns Hopkins Drug Discovery, Johns Hopkins University, Baltimore, Maryland 21205, United States
- Camilo Rojas** – Johns Hopkins Drug Discovery, Johns Hopkins University, Baltimore, Maryland 21205, United States
- Hiroe Hihara** – Tsukuba Research Laboratories, Eisai Co., Ltd., Tsukuba, Ibaraki 300-2635, Japan
- Mika Aoki** – Tsukuba Research Laboratories, Eisai Co., Ltd., Tsukuba, Ibaraki 300-2635, Japan
- Kyoko Yoshizawa** – Tsukuba Research Laboratories, Eisai Co., Ltd., Tsukuba, Ibaraki 300-2635, Japan
- Tomoki Nishioka** – Tsukuba Research Laboratories, Eisai Co., Ltd., Tsukuba, Ibaraki 300-2635, Japan
- Shuichi Suzuki** – Tsukuba Research Laboratories, Eisai Co., Ltd., Tsukuba, Ibaraki 300-2635, Japan
- Shao-Qiu He** – Department of Anesthesiology and Critical Care Medicine, Johns Hopkins University, Baltimore, Maryland 21205, United States
- Qi Peng** – Solomon H. Snyder Department of Neuroscience, Johns Hopkins University, Baltimore, Maryland 21205, United States
- Yun Guan** – Department of Anesthesiology and Critical Care Medicine, Johns Hopkins University, Baltimore, Maryland 21205, United States
- Xinzhong Dong** – Solomon H. Snyder Department of Neuroscience, Johns Hopkins University, Baltimore, Maryland 21205, United States
- Srinivasa N. Raja** – Department of Anesthesiology and Critical Care Medicine, Johns Hopkins University, Baltimore, Maryland 21205, United States
- Barbara S. Slusher** – Johns Hopkins Drug Discovery, Department of Neurology, and Solomon H. Snyder Department of Neuroscience, Johns Hopkins University, Baltimore, Maryland 21205, United States; orcid.org/0000-0001-9814-4157

Complete contact information is available at: <https://pubs.acs.org/doi/10.1021/acs.jmedchem.1c01709>

Author Contributions

All authors have contributed to the work and have given approval to the final version of the manuscript.

Notes

The authors declare no competing financial interest.

ACKNOWLEDGMENTS

This research was supported by NIH grants UG3NS115718 (T.T.), R21NS101954 (T.T.), R01NS054791 (X.D.), R01NS070814 (Y.G.), R01NS117761 (Y.G.), R01NS110598 (Y.G.), T32NS070201 (I.B.), and the Johns Hopkins Institute for Clinical and Translational Research (ICTR), which was funded in part by UL1TR001079 from the National Center for Advancing Translational Sciences (NCATS). X.D. is an investigator of the Howard Hughes Medical Institute. Animal behavioral studies were facilitated by the Pain Research Core funded by the Blaustein Fund and the Neurosurgery Pain Research Institute at the Johns Hopkins University.

ABBREVIATIONS

MRGPRX1, Mas-related G-protein-coupled receptor member X1; DRG, dorsal root ganglion; HTS, high-throughput screening; CCI, chronic constriction injury

REFERENCES

- (1) Dong, X.; Han, S.; Zylka, M. J.; Simon, M. I.; Anderson, D. J. A diverse family of gpcrs expressed in specific subsets of nociceptive sensory neurons. *Cell* **2001**, *106*, 619–632.
- (2) Lembo, P. M.; Grazzini, E.; Groblewski, T.; O'Donnell, D.; Roy, M. O.; Zhang, J.; Hoffert, C.; Cao, J.; Schmidt, R.; Pelletier, M.; Labarre, M.; Gosselin, M.; Fortin, Y.; Banville, D.; Shen, S. H.; Strom, P.; Payza, K.; Dray, A.; Walker, P.; Ahmad, S. Proenkephalin a gene products activate a new family of sensory neuron-specific gpcrs. *Nat. Neurosci.* **2002**, *5*, 201–209.
- (3) Chen, H.; Ikeda, S. R. Modulation of ion channels and synaptic transmission by a human sensory neuron-specific g-protein-coupled receptor, *snsr4/mrgx1*, heterologously expressed in cultured rat neurons. *J. Neurosci.* **2004**, *24*, 5044–5053.
- (4) Li, Z.; He, S. Q.; Xu, Q.; Yang, F.; Tiwari, V.; Liu, Q.; Tang, Z.; Han, L.; Chu, Y. X.; Wang, Y.; Hin, N.; Tsukamoto, T.; Slusher, B.; Guan, X.; Wei, F.; Raja, S. N.; Dong, X.; Guan, Y. Activation of *mrgc* receptor inhibits n-type calcium channels in small-diameter primary sensory neurons in mice. *Pain* **2014**, *155*, 1613–1621.
- (5) Wilson, S. R.; Gerhold, K. A.; Bifolck-Fisher, A.; Liu, Q.; Patel, K. N.; Dong, X.; Bautista, D. M. *Trpa1* is required for histamine-independent, mas-related g protein-coupled receptor-mediated itch. *Nat. Neurosci.* **2011**, *14*, 595–602.
- (6) Wroblowski, B.; Wigglesworth, M. J.; Szekeres, P. G.; Smith, G. D.; Rahman, S. S.; Nicholson, N. H.; Muir, A. I.; Hall, A.; Heer, J. P.; Garland, S. L.; Coates, W. J. The discovery of a selective, small molecule agonist for the mas-related gene *x1* receptor. *J. Med. Chem.* **2009**, *52*, 818–825.
- (7) Prchalová, E.; Hin, N.; Thomas, A. G.; Veeravalli, V.; Ng, J.; Alt, J.; Rais, R.; Rojas, C.; Li, Z.; Hihara, H.; Aoki, M.; Yoshizawa, K.; Nishioka, T.; Suzuki, S.; Kopajtic, T.; Chatrath, S.; Liu, Q.; Dong, X.; Slusher, B. S.; Tsukamoto, T. Discovery of benzamidine- and 1-aminoisoquinoline-based human mas-related g-protein-coupled receptor *x1* (*mrgprx1*) agonists. *J. Med. Chem.* **2019**, *62*, 8631–8641.
- (8) Li, Z.; Tseng, P. Y.; Tiwari, V.; Xu, Q.; He, S. Q.; Wang, Y.; Zheng, Q.; Han, L.; Wu, Z.; Blobaum, A. L.; Cui, Y.; Tiwari, V.; Sun, S.; Cheng, Y.; Huang-Lionnet, J. H.; Geng, Y.; Xiao, B.; Peng, J.; Hopkins, C.; Raja, S. N.; Guan, Y.; Dong, X. Targeting human mas-related g protein-coupled receptor *x1* to inhibit persistent pain. *Proc. Natl. Acad. Sci. U.S.A.* **2017**, *114*, E1996–E2005.
- (9) Wen, W.; Wang, Y.; Li, Z.; Tseng, P. Y.; McManus, O. B.; Wu, M.; Li, M.; Lindsley, C. W.; Dong, X.; Hopkins, C. R. Discovery and

characterization of 2-(cyclopropanesulfonamido)-n-(2-ethoxyphenyl)-benzamide, *ml382*: A potent and selective positive allosteric modulator of *mrgx1*. *ChemMedChem* **2015**, *10*, 57–61.

(10) Woszczek, G.; Fuerst, E. Ca²⁺ mobilization assays in gpcr drug discovery. *Methods Mol. Biol.* **2015**, *1272*, 79–89.

(11) Shi, T.; Kaneko, L.; Sandino, M.; Busse, R.; Zhang, M.; Mason, D.; Machulis, J.; Ambrose, A. J.; Zhang, D. D.; Chapman, E. One-step synthesis of thieno[2,3-d]pyrimidin-4(3h)-ones via a catalytic four-component reaction of ketones, ethyl cyanoacetate, s8 and formamide. *ACS Sustainable Chem. Eng.* **2019**, *7*, 1524–1528.

(12) Pubchem identifier: Aid 602413. <https://pubchem.ncbi.nlm.nih.gov/bioassay/602413>.

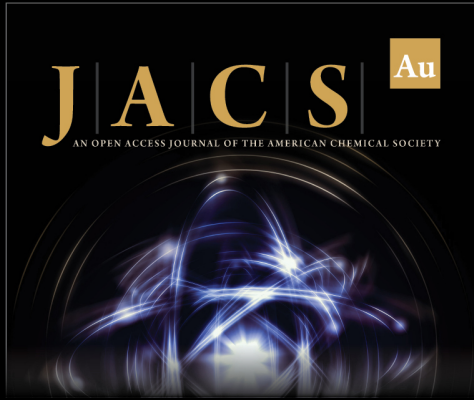
(13) McNeil, B. D.; Pundir, P.; Meeker, S.; Han, L.; Udem, B. J.; Kulka, M.; Dong, X. Identification of a mast-cell-specific receptor crucial for pseudo-allergic drug reactions. *Nature* **2015**, *519*, 237–241.

(14) Bowes, J.; Brown, A. J.; Hamon, J.; Jarolimek, W.; Sridhar, A.; Waldron, G.; Whitebread, S. Reducing safety-related drug attrition: The use of in vitro pharmacological profiling. *Nat. Rev. Drug Discovery* **2012**, *11*, 909–922.

(15) Bennett, G. J.; Xie, Y. K. A peripheral mononeuropathy in rat that produces disorders of pain sensation like those seen in man. *Pain* **1988**, *33*, 87–107.

(16) Taylor, S.; Murfin, S.; Coulter, T. S.; Jaekel, S.; Aicher, B.; Kelter, A.-R.; Krämer, J.; Kirchoff, C.; Scheel, A.; Wölcke, J. Thienopyrimidines for Pharmaceutical Compositions. WO Patent WO2006/1364022006.

(17) Giancola, J. B.; Bonifazi, A.; Cao, J.; Ku, T.; Haraczy, A. J.; Lam, J.; Rais, R.; Coggiano, M. A.; Tanda, G.; Newman, A. H. Structure-activity relationships for a series of (bis(4-fluorophenyl)methyl)-sulfinyethyl-aminopiperidines and -piperidine amines at the dopamine transporter: Bioisosteric replacement of the piperazine improves metabolic stability. *J. Med. Chem.* **2020**, *208*, No. 112674.



JACS Au
AN OPEN ACCESS JOURNAL OF THE AMERICAN CHEMICAL SOCIETY

Editor-in-Chief
Prof. Christopher W. Jones
Georgia Institute of Technology, USA

Open for Submissions

pubs.acs.org/jacsau ACS Publications
Most Trusted. Most Cited. Most Read.